Analysis & Sensing

Concept
doi.org/10.1002/anse.202200028

Chemistry Europe
European Chemical
Societies Publishing

www.analysis-sensing.org

Design and Testing of Diagnostic MRI/MRS Applications Based On Signal Enhancement by Parahydrogen-Induced Polarization

Francesca Reineri*[a]

Parahydrogen-induced polarization is a hyperpolarization method that exploits the spin order of hydrogen enriched in the *para*-isomer, by means of a chemical reaction. Recently, its field of application has been extended significantly, through the introduction of non-hydrogenative PHIP (i.e. SABRE) and of innovative h-PHIP strategies that allowed to increase the intensity of the MR signals in molecules relevant for biological applications. This Concept article aims to show the potentialities of this hyperpolarization method in the field of diagnostics, through the discussion of some of the reported applications of parahydrogen polarized substrates. A section is also dedicated to the methods that have been introduced for the purification of parahydrogen polarized products, in order to make them suitable for biological studies.

1. Introduction

The introduction of methods for hyperpolarizing nuclear spins in solution, in particular of parahydrogen induced polarization (PHIP)[1] and dissolution-dynamic nuclear polarization (d-DNP),[2,3] increased the sensitivity of the ^{13}C (and other nuclei) NMR detection by several thousands of times. This allowed the detection of molecules at millimolar concentration in biological systems, on the timescale of a few seconds. PHIP polarized substrates have been investigated since the early 2000s, when the first in-vivo studies using hyperpolarized liquid substrates have been published.[4,5] Then, the diagnostic applications of hyperpolarized (HP) molecules in solution have been developed quickly thanks to d-DNP.

D-DNP is a versatile and powerful hyperpolarization technique that can increase the sensitivity of, in principle, any molecule. The wealth of chemical information that MRI and MRS can provide, in the characterization of biological tissues, non-invasively, is unique and ^{13}C MRS is potentially the most useful technique for monitoring tissues metabolism and its alterations in diseases. The access to d-DNP hyperpolarized metabolites has made possible the investigation of metabolic pathways in-vivo, in real time. Nevertheless, its use is limited due to the high costs of purchase and maintenance, to the technical complexity and the long hyperpolarization cycles of this technology.

PHIP is a cheap hyperpolarization method, less technically demanding than d-DNP and the basic equipment needed to carry out experiments using para-enriched hydrogen can be easily found in a chemistry laboratory.[6] It allows hyperpolarization cycles at significantly faster pace, but its field of application appeared quite limited, at least in the first two decades since its discovery.[7,8] This is due to the fact that hydrogenative-PHIP (h-PHIP) relies on the addition of a hydrogen molecule to an unsaturated substrate, therefore, only those molecules for which an unsaturated precursor (alkyne or alkene) exists, seemed suitable for this hyperpolarization method.

In 2009, the scope of parahydrogen based hyperpolarization widened significantly thanks to the introduction of the non-hydrogenative method SABRE (Signal Amplification by Reversible Exchange), that does not imply any chemical modification of the substrate. Recently, the use of h-PHIP has been expanded too, making possible the hyperpolarization of metabolites, such as pyruvate and fumarate[9,10] and the interest in PHIP based hyperpolarization is increasing.

In the following paragraphs, the fundamentals of parahydrogen hyperpolarization will be presented and the potential applications of PHIP polarized molecules to diagnostics in-vivo and in-vitro will be described.

2. Hyperpolarization from parahydrogen

The combination of two magnetically equivalent nuclear spins $^1/_2$ leads to the formation of the four nuclear spin states (Eq. 1)

$$|\alpha\alpha\rangle,\ |\beta\beta\rangle,\ \frac{1}{\sqrt{2}}(|\alpha\beta\rangle + |\beta\alpha\rangle)\ \text{and}\ \frac{1}{\sqrt{2}}(|\alpha\beta\rangle - |\beta\alpha\rangle) \tag{1}$$

The first three states have a total spin angular momentum $I = +1$ and form a triplet state, while the fourth state has a total spin angular momentum $I = 0$ and is a singlet state.

[a] Prof. F. Reineri
Department of Molecular Biotechnology and Health Sciences
University of Torino
Via Nizza 52
10126 Torino (Italy)
E-mail: francesca.reineri@unito.it
Homepage: https://www.cim.unito.it/website/PI/Reineri/home.php

These states are often referred to using the singlet-triplet notation, (Eq. 2)

$$|T_+\rangle = |\alpha\alpha\rangle, \tag{2a}$$

$$|T_0\rangle = \frac{1}{\sqrt{2}}(|\alpha\beta\rangle + |\beta\alpha\rangle) \tag{2b}$$

$$|T_-\rangle = |\beta\beta\rangle \tag{2c}$$

$$|S_0\rangle = \frac{1}{\sqrt{2}}(|\alpha\beta\rangle - |\beta\alpha\rangle) \tag{2d}$$

where the subscript refers to the eigenvalue of the total square spin angular momentum operator ($I^2 = I_x^2 + I_y^2 + I_z^2$) of each state, for example $I^2|S_0\rangle = 0$.

The singlet state is not coupled with the triplet states due to different symmetry, in fact the triplet states are symmetric, while the singlet state is antisymmetric upon exchange of the two spins. In the case of hydrogen gas, the para and ortho spin isomers are so well isolated that they form two physically different substances, named parahydrogen and orthohydrogen, respectively.[11]

At room temperature, all the four nuclear spin states are equally populated, giving 25% of the para-form. Since the para state is the most stable one, the fraction of parahydrogen increases when the temperature is lowered being almost 100% at ~20 K. Nevertheless, symmetric interactions of the two spins (e.g. intramolecular dipole-dipole interactions) cannot couple the singlet and the triplet states, bringing into equilibrium the population of the two forms of hydrogen, due to their different symmetry. Therefore inhomogeneous interactions, such as those on the surface of a catalyst, are needed to reach the thermal equilibrium.[12] It follows that the enrichment in the para-isomer obtained at low temperature can be maintained at high temperature (room temperature or higher) provided that the conversion catalyst is removed. This non-equilibrium mixture is termed parahydrogen and contains a high spin order that can be converted into hyperpolarization.[7,8,13]

Parahydrogen is magnetically inactive (the magnetic momentum is zero) and hyperpolarization can be obtained if its symmetry is broken by means of a chemical transformation that leads to chemically or magnetically inequivalent spins.

In Hydrogenative PHIP, a hydrogen molecule is added to an unsaturated substrate (usually an alkene or alkyne) in a pairwise manner, i.e. the spin correlation between the two hydrogen nuclei is maintained. The hydrogenation reaction has also to be fast, in the timescale of the relaxation processes, because the spin states population tends to the thermal equilibrium, once that the symmetry of the hydrogen molecule is broken and the singlet state is lost.

In non-hydrogenative PHIP (SABRE),[14] the latent magnetization of parahydrogen is catalytically transferred to a substrate in reversible exchange on a metal complex (usually an iridium Crabtree-like complex) (Figure 1). The metal center works as a molecular scaffold that brings together the hydrogen molecule and the substrate. It follows that the main
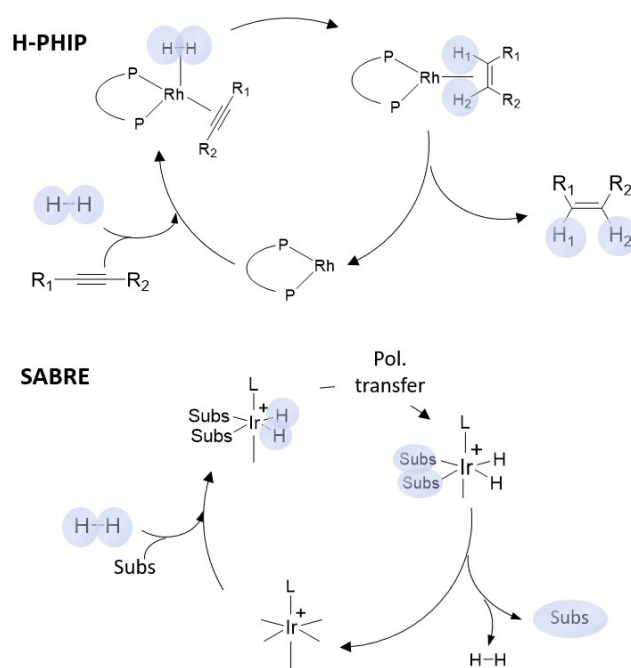

Figure 1. Top: a generic example of hydrogenative-PHIP. Parahydrogen is added, by means of a hydrogenation catalyst (Rh(I)diphos complexes are usually applied), to an alkyne. Spin order is transferred to the alkene thus obtained. Bottom: example of SABRE hyperpolarization of a generic substrate (Subs) through the formation of a ternary adduct between with an Ir(I) complex (L=PCy$_3$ or L=Imes = 1,3-bis(2,4,6-trimethylphenyl)imidazol-2-ylidine[17]) and parahydrogen. Notice that, in SABRE, the chemical structure of the substrate is not changed, while in h-PHIP the hyperpolarized product incorporates the parahydrogen molecule.

requirement, for a SABRE substrate, is the capability of binding to the iridium complex. The most commonly used substrates are heterocycles containing an electro-donating atom, typically nitrogen.[15] The process is completed without any chemical change of the substrate, is continuous and refreshable.[16]

The easiest way to describe how parahydrogen can lead to hyperpolarization of the ^{1}H-NMR signals, in an h-PHIP experiment, relies on the calculation of the population of the nuclear spin states[18] of a molecule formed upon the addition of parahydrogen to an unsaturated bond (Figure 2).

Following to the addition of hydrogen to the substrate, the spin states of hydrogen (Eq. 2)$|S_0\rangle$, $|T_+\rangle$, $|T_0\rangle$, $|T_-\rangle$) change instantaneously into the states of the product molecule. For sake of completeness, it must be said that this is an ideal situation, because the hydrogenation catalyst has an effect on the singlet state and singlet-triplet mixing occurs on hydrogenation intermediates. Nevertheless, this so-called sudden approximation is often used in the description of h-PHIP experiments. The spin states of the two protons on the product can be conveniently written as a combination of the singlet-triplet states as reported in Eq. 3:[20]

$$\psi_1 = |T_+\rangle = |\alpha\alpha\rangle \tag{3a}$$

$$\psi_2 = \cos\left(\frac{\theta}{2}\right)|\alpha\beta\rangle + \sin\left(\frac{\theta}{2}\right)|\beta\alpha\rangle \tag{3b}$$
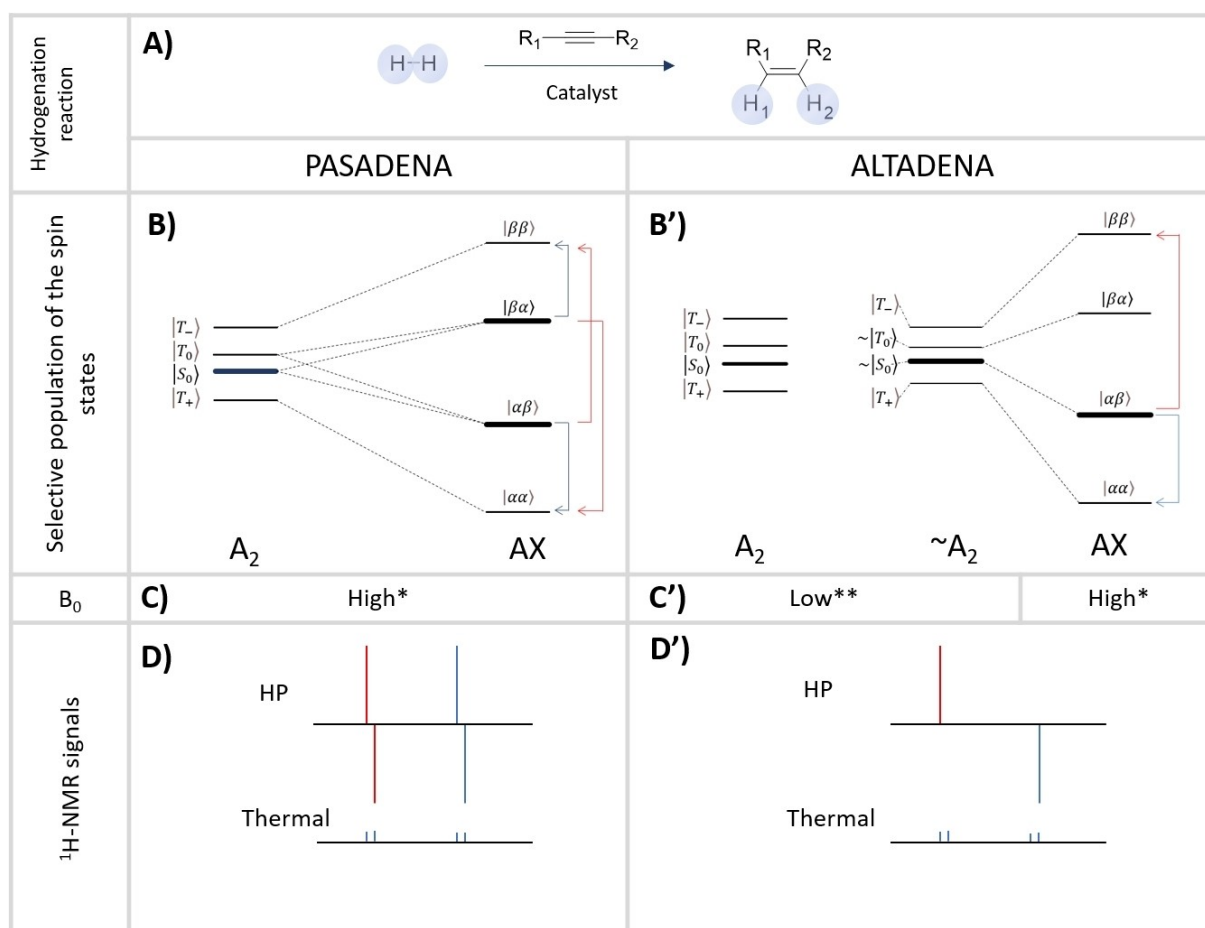
Figure 2. The two variants of the hydrogenative-PHIP experiments (PASADENA and ALTADENA). A) Hydrogen addition to a triple bond, on an asymmetric substrate ($R_1 \neq R_2$), leading to two chemically different protons (H_1 and H_2). B) in a PASADENA experiment, the hydrogenation reaction takes place at high field (such that $|\nu_A - \nu_X| \gg J_{AX}$) and an AX system is "suddenly" formed, having the spin states $\alpha\alpha$, $\alpha\beta$, $\beta\alpha$ and $\beta\beta$. Only those states that overlap with the para-state are more populated (thick lines) while the other states are less populated (thin lines). Consequently, four intense NMR transitions are possible from these states, as shown by the red and blue arrows and schematized in D. B') In an ALTADENA experiment the reaction takes place in the fringe field of the NMR magnet (i.e. $|\nu_A - \nu_X| \ll J$) and the spin states are little changed, so the parahydrogen state adds predominantly into the product state with the singlet character. After the hydrogenation reaction, the parahydrogenated sample is transferred into the high field of the NMR magnet for rf irradiation and detection and the AX system is obtained. The passage from low to high field must be rapid with respect to the spin-lattice relaxation to preserve the spin order, but also sufficiently slow that the population of the singlet-like low field eigenstate is transferred adiabatically into the high-field eigenstate with which it correlates with continuity,[19] as shown in the correlation diagram. As a result, in-phase signals are obtained for each proton, while antiphase signals were observed in the PASADENA experiment (see D and D').

$$\psi_3 = \sin\left(\frac{\theta}{2}\right)|\alpha\beta\rangle - \cos\left(\frac{\theta}{2}\right)|\beta\alpha\rangle \qquad (3c)$$

$$\psi_4 = |T_-\rangle = |\beta\beta\rangle . \qquad (3d)$$

The mixing angle θ depends on the scalar coupling between the two protons and on their frequency difference $\tan(\theta) = \frac{J_{H1H2}}{\nu_{H1} - \nu_{H2}}$.

When the frequency difference ($\nu_{H1} - \nu_{H2}$) tends to zero, the ψ_3 state (Eq. 3c) corresponds to the parahydrogen state, therefore this is the only state that becomes more populated. This is the ALTADENA condition,[19] in which the reaction occurs at low magnetic field (usually at the geomagnetic field), where the chemical shift difference between protons is neglectable and they resonate at the same Larmor frequency. Following an adiabatic (i.e. slow) transport of the sample into the high field

of the NMR spectrometer, the population of the states is maintained and hyperpolarization results into in-phase signals (hyperpolarized net magnetization) (Figure 2).

Vice-versa, when the frequency difference between the two protons is significantly larger than their mutual scalar coupling (($\nu_{H1} - \nu_{H2}$) $\gg J_{HH}$), i.e. in the weak coupling condition, the states $\psi_2 = |\alpha\beta\rangle$ and $\psi_3 = |\beta\alpha\rangle$ are formed, which are equally populated because they both connect with the parahydrogen state. This situation occurs in the PASADENA experiments and hyperpolarized antiphase signals are obtained for the two protons (Figure 2).

In practice, ^1H hyperpolarization is not usually applied for in-vivo MRI studies, due to the large background signal of water protons and to the relaxation rate of ^1H, that limits the lifetime of the HP signals to few seconds. Heteronuclear signals, and in particular ^{13}C resonances, are usually preferred, because of the large chemical shift range, the lack of background signals

and the longer T_1, especially in some functional groups such as the carboxylate group.

Hyperpolarization can be transferred spontaneously from parahydrogen protons to heteronuclei through the scalar couplings. Let's consider the simplest case in which a heteronucleus (X) is added to the two protons spin states and an A_2X system is formed. The eigenstates are the product of the singlet/triplet states for the two protons and the α and β state for the heteroatom (Eq. 4)

$$|T_+\alpha\rangle = |\alpha\alpha\alpha\rangle, \ |T_+\beta\rangle = |\alpha\alpha\beta\rangle, \tag{4a}$$

$$|S_0\alpha\rangle = \frac{1}{\sqrt{2}}|(\alpha\beta - \beta\alpha)\alpha\rangle, \ |S_0\beta\rangle = \frac{1}{\sqrt{2}}|(\alpha\beta - \beta\alpha)\beta\rangle, \tag{4b}$$

$$\left|T_0\alpha\right\rangle = \frac{1}{\sqrt{2}}|(\alpha\beta + \beta\alpha)\alpha\rangle, \ |T_0\beta\rangle = \frac{1}{\sqrt{2}}|(\alpha\beta + \beta\alpha)\beta\rangle, \tag{4c}$$

$$|T_-\alpha\rangle = |\beta\beta\alpha\rangle, \ |T_-\beta\rangle = |\beta\beta\beta\rangle \tag{4d}$$

In this case, only the states $|S_0\alpha\rangle$ and $|S_0\beta\rangle$ are populated and, being transitions from these states forbidden, hyperpolarization is not observed. Vice-versa, when the two protons are added to magnetically different sites, an AA'X spin system is formed, thanks to asymmetric coupling of the two protons with ^{13}C (Figure 3).[21] In this case, the spin states can be written, using the singlet-triplet-Zeeman basis[22] as in Eq. 5:

$$\psi_1 = |T_+\alpha\rangle, \ \psi_2 = |T_+\beta\rangle \tag{5a}$$

$$\psi_3 = |S'_0\alpha\rangle = \cos\left(\frac{\theta_G}{2}\right)|\beta\alpha\alpha\rangle - \sin\left(\frac{\theta_G}{2}\right)|\alpha\beta\alpha\rangle, \tag{5b}$$

$$\psi_4 = |T'_0\alpha\rangle = \cos\left(\frac{\theta_G}{2}\right)|\alpha\beta\alpha\rangle + \sin\left(\frac{\theta_G}{2}\right)|\beta\alpha\alpha\rangle, \tag{5c}$$
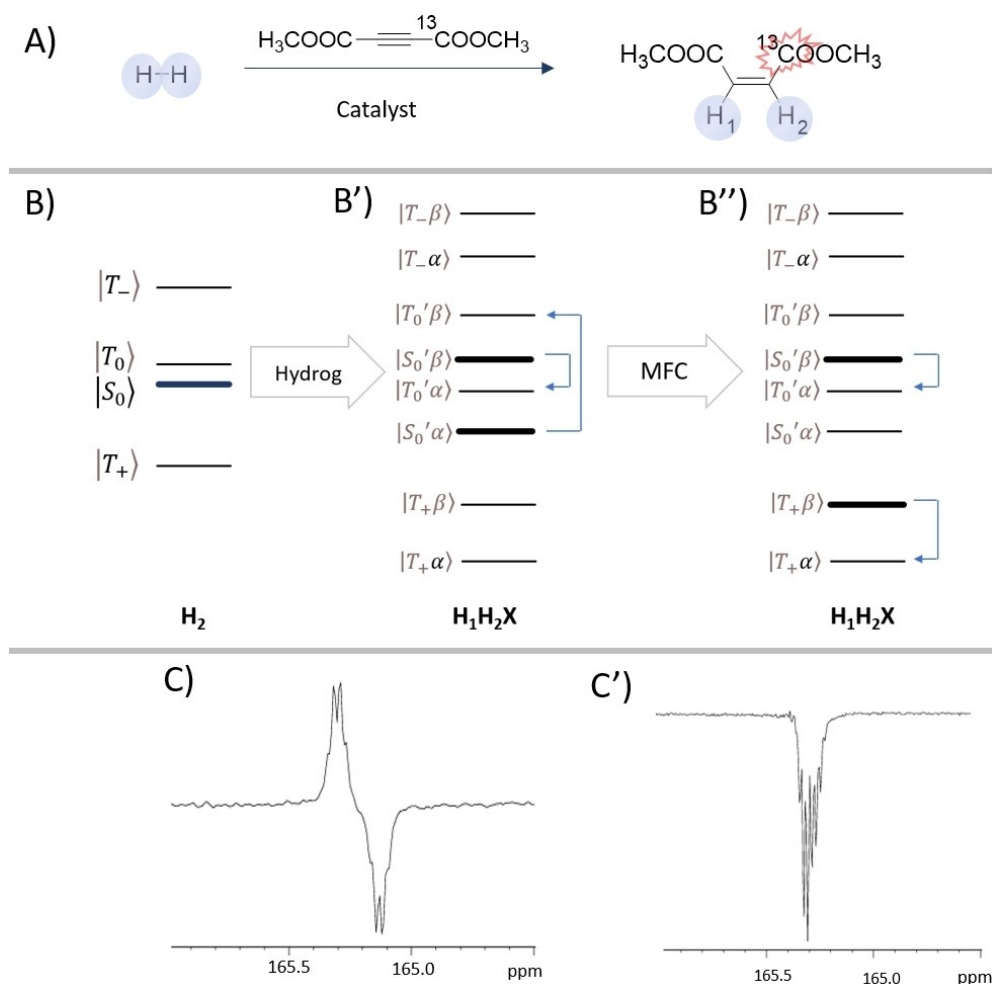

Figure 3. A) Parahydrogen is added to dimethyl-[1-^{13}C] acetylene dicarboxylate. The cis-addition is catalyzed by the [Rhdppb]$^+$ complex (dppb = bis-diphenylphosphino butane) that is more usually applied for h-PHIP. In the product molecule dimethyl-maleate, a three-spins system is formed (H_1H_2X). B) Population of the nuclear spin states before the hydrogenation reaction (H_2 enriched in para-isomer): the bold-faced line represent the more populated state (para-state). B') After hydrogen addition to the triple bond, the H_1H_2X spin system is formed and two states are more populated (bold-faced lines). Transitions from these two states to the other, thermally populated states, are hyperpolarized (blue arrows): an antiphase signal is observed for ^{13}C (C). B'') Population of the nuclear spin states after the application of MFC,[23] now the hyperpolarized transitions (blue arrows) are in-phase (emission signal, C'). C and C' are the ^{13}C hyperpolarized signals before and after the application of MFC, respectively.

$$\psi_5 = |S'_0\beta\rangle = \cos\left(\frac{\theta_G}{2}\right)|\alpha\beta\beta\rangle - \sin\left(\frac{\theta_G}{2}\right)|\beta\alpha\beta\rangle, \quad (5d)$$

$$\psi_6 = |T'_0\beta\rangle = \cos\left(\frac{\theta_G}{2}\right)|\beta\alpha\beta\rangle + \sin\left(\frac{\theta_G}{2}\right)|\alpha\beta\beta\rangle, \quad (5e)$$

$$\psi_7 = |\beta\beta\alpha\rangle, \ \psi_8 = |\beta\beta\beta\rangle \quad (5f)$$

Of the eight states thus obtained, four derive from mixing of the states $|S_0\alpha\rangle$ and $|T_0\alpha\rangle$ (total spin $-1/2$), $|S_0\beta\rangle$ and $|T_0\beta\rangle$ (total spin $1/2$) and the mixing angle is

$$\theta_G = \arctan\frac{2\omega_{H_1H_2}}{\omega^{\Delta}_{H_1H_2X}} \text{ with } \omega_{H_1H_2} = 2\pi J_{H_1H_2} \text{ and } \omega^{\Delta}_{H_1H_2X} = \\ 2\pi\left(J_{H_1X} - J_{H_2X}\right) \quad (6)$$

The percentage of singlet of the states ψ_3, ψ_4, ψ_5 and ψ_6 is a function of the J-couplings involved.

When the two H–X coupling are equal, the system is symmetric and the states correspond to pure singlet-Zeeman and triplet-Zeeman states. Otherwise, when the two J couplings (J_{H1X} and J_{H2X}) are different, the heteronuclear transitions $\psi_3 \rightarrow \psi_6$ and $\psi_4 \rightarrow \psi_5$ have non-null probability and are hyperpolarized (Figure 3), leading to hyperpolarized anti-phase signals on ^{13}C (i.e. hyperpolarized ^1H-^{13}C spin order) and the net magnetization on the heteroatom is zero.(Figure 3) Spin order can be converted into net magnetization (Figure 3) through the application of magnetic field cycling,[5,23] as reported by K.Golman in the first in-vivo application of a hyperpolarized substrate. Other methods have been reported to achieve this goal, based on the application of rf pulses.[24–27]

3. Advances in PHIP-based methods

3.1. PHIP based agents for angiography and perfusion imaging

Magnetic Resonance Angiography is an important method for diagnosing various medical conditions and it may take advantage from the use of vasculature contrast agents such as blood pool agents.[28] MR-based approaches to quantify perfusion make use of injection of relaxation-based MR contrast media or use magnetic spin labeling techniques. These approaches suffers from limitations, in particular, some Gd-based CAs have been suspended in Europe because of major concerns associated to long-term accumulation of Gd containing species in the patients' bodies.[29] On the other hand, the arterial spin labeling approaches are limited by ^1H longitudinal relaxation.

The strong signal of hyperpolarized spins allows the direct detection of hyperpolarized molecules and, in the first in-vivo application of hyperpolaried liquids, hydroxyethyl propionate (HEP) polarized by means of h-PHIP was used for catheter tracking and angiography.[5,30] In that case, the polarization level was in the order of 25–30%, an aqueous solution was obtained directly from the hydrogenation reaction carried out in water

and the concentration of the agent was 0.5–1 M. Although the toxicity profile of HEP did not make it suitable for clinical translation, the contrast capacity of this new method for angiographic examination was successfully demonstrated and also it showed to be suitable to provide perfusion data about the myocardium in pigs.[5]

Succinate is a metabolite that takes part into the TCA cycle, i.e. it is central in the metabolic energy production. However, since transport of dicarboxylic acids across biological membranes is quite limited, real time metabolism has not been observed using this hyperpolarized substrate. Anyhow, its biocompatibility should make it suitable as a tracer for angiography and perfusion. Hyperpolarized [1-^{13}C]succinate has been obtained, first, by means of parahydrogenation of sodium acetylene dicarboxylate,[31] and later from parahydrogen addition to 1-^{13}C-fumaric acid-d_2.[32] In the second case, the choice of a deuterated precursor maximizes the T_1 for the hyperpolarized product. The polarization level was 15–20% and the concentration of the hyperpolarized molecule was 3–4 mM. The parahydrogenation was carried out in aqueous solution, using a water-soluble rhodium catalyst and a dedicated instrumentation for parahydrogen addition and transfer of spin order.[33] Another route to obtain the same product has been reported, using ^{13}C labelled maleic anhydride as a precursor.[34] In this case, the use of a lipophilic substrate allowed to carry out the hydrogenation reaction in an organic hydrophobic solvent. Following to the spin order transfer to ^{13}C of the parahydrogenated anhydride, the aqueous solution of the hyperpolarized succinic acid was obtained by means of the fast hydrolysis of the anhydride and extraction of the product in in the aqueous phase. The liquid-liquid extraction of the HP agent corresponds also to the purification step, as will be discussed in a following section.

Another molecule that has to be considered in this context is ^{13}C-urea, as it is not taken up and metabolized by most tissues. It has been shown that hyperpolarized urea, obtained by means of the d-DNP method, provides accurate assessment of blood perfusion in animal cancer models.[35] Hyperpolarization of this substrate has been obtained also by using SABRE-RELAY.[36] This variant of SABRE relies on the non-hydrogenative PHIP of a transfer reagent (ammonia) and the subsequent relay of hyperpolarization to the analyte of interest, though fast proton exchange. This method allowed to extend the application of PHIP quite significantly, to different classes of compounds (carboxylic acids, alcohols, phosphates, glucose) further than urea (^{13}C and ^{15}N labelled). However the attained polarization level is still rather low ($< 0.5\%$) and further improvements of the method are necessary to make it suitable for in-vivo applications. Another issue deals with the solvent in which HP-urea is obtained (i.e. CD_2Cl_2), that is not compatible with biological studies.

3.2. PHIP polarized substrates for metabolic imaging

The most relevant application of hyperpolarized substrates in the diagnostic field is the assessment of metabolic processes

in-vivo. Although many metabolites have been hyperpolarized by means of d-DNP,[37] only a handful of them have been successfully applied for these studies. Pyruvate is the most widely used for the investigation of different diseases, and the first translated to the clinic.[38,39] This molecule is at the crossroads of different metabolic processes, as it is transformed into lactate by the cytoplasmatic LDH (lactate dehydrogenase), into alanine by alanine transaminase (ALT) and enters the TCA cycle thanks to decarboxylation by means of pyruvate decarboxylase.

Hyperpolarization of pyruvate has been pursued by means of both hydrogenative and non-hydrogenative PHIP based techniques.

Using the SABRE method, the issue of the poor coordination of pyruvate to the iridium complex Ir(COD)(NHC)Cl (NHC = IMes)[40,41] had to be solved. This task was tackled by tuning the coordination capacity of the metal center by means of different ligands. It was observed that the addition of DMSO (or its derivatives) allows to obtain an unstable intermediate [Ir-(H)$_2$(DMSO)$_2$Imes] that forms [Ir(H)$_2$(η^2-pyruvate)(sulfoxide)].[42] In SABRE, the hyperpolarization level results from complex interplay between different factors, in particular the catalyst identity, the substrate and co-substrate concentration, temperature and solvent properties.[43] The best conditions for SABRE polarization of pyruvate brought to 1.7% ^{13}C polarization on the free molecule, while ~13% polarization has been observed as total polarization for free and coordinated pyruvate, at low temperature.[44]

By using the SABRE polarized [1,2-^{13}C$_2$]pyruvate, it was possible to observe its chemical transformation into CO$_2$ and ethanolic acid, through the reaction with hydrogen peroxide.[45]

The h-PHIP approach to pyruvate hyperpolarization makes use of the SAH (Side Arm Hydrogenation) method,[9] which relies on the functionalization of the carboxylate group with an unsaturated alcohol, to yield an ester derivative of pyruvate containing the unsaturated group on the alcoholic moiety. Hyperpolarization is obtained through the following steps: a) hydrogenation of the unsaturated side-arm using p-H$_2$; b) spin order transfer from the parahydrogen protons to the ^{13}C carboxylate spin; c) cleavage of the hydrogenated alcohol by means of hydrolysis. Hydrogenation is carried out in an hydrophobic solvent (e.g. chloroform or toluene[46]) and the use of an aqueous base for hydrolysis leads to the separation of two phases. The catalyst is retained in the organic phase, while the carboxylate salt is extracted in the aqueous one. The aqueous solutions of HP metabolite thus obtained have been used for metabolic investigations in-vivo[47] and in-cells[48,49] (Figure 4). The SAH method can be applied, in principle, to any substrate containing a carboxylate group such as acetate,[50] lactate,[51] amino acids.[52,53] Concerning the hyperpolarization of AAs, it should be mentioned that also other PHIP-based
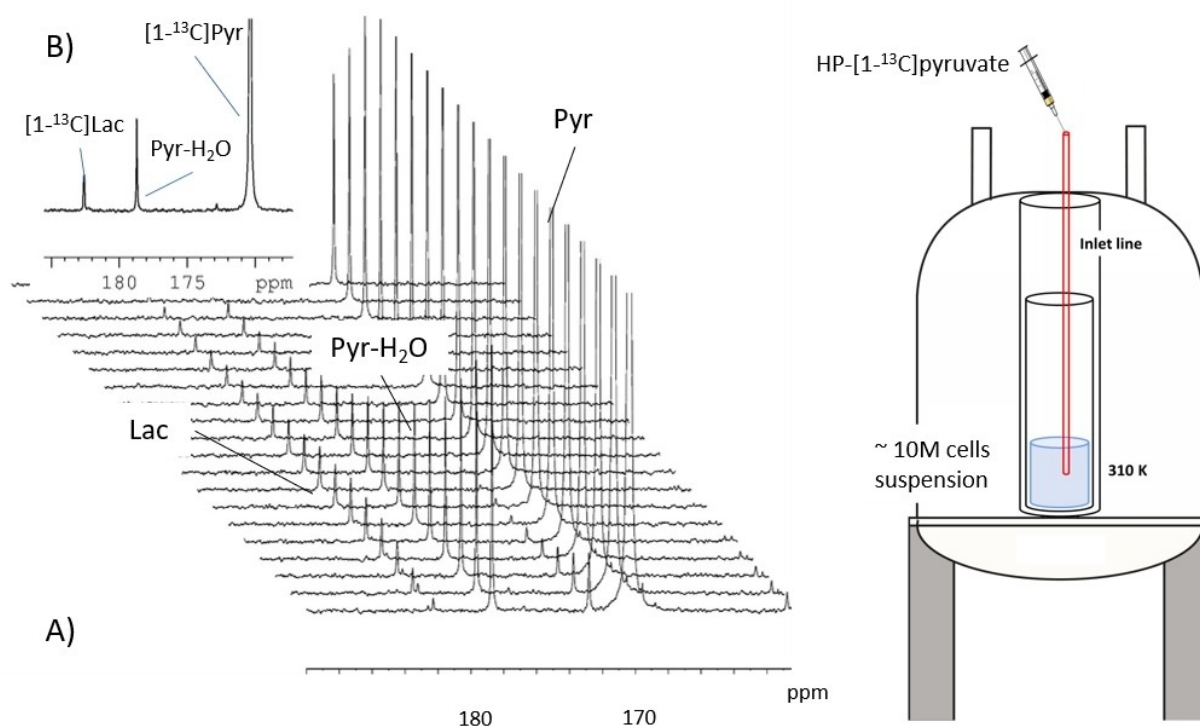

Figure 4. A) time-resolved ^{13}C-NMR spectra (20° flip angle, 2 s inter-scan delay) acquired following to the perfusion of HP-[1-^{13}C]pyruvate (5 mM) through prostate cancer cells (10 M PC3 cells) suspended in their growth medium. The build-up of the [1-^{13}C]lactate signal can be observed, due to the metabolic conversion of the injected pyruvate. The setup for perfusion of the HP metabolite through the cells is shown on the right: cells are placed inside the NMR spectrometer and the temperature is set to 310 K, before the addition of the HP metabolite. The stacked plot of ^{13}C-NMR spectra is reproduced from ref [49], copyright (2020), with permission of the Publisher (article distributed under the terms of the Creative Commons Attribution License (CC BY)).

methods have been used, from the direct h-PHIP of dehydrogenated precursors (dehydro-AAs)[54] to SABRE.[55]

D-DNP studies showed that HP $[1,4-^{13}C_2]$fumarate can be used as a reporter of necrosis, being transformed into $[1,4-^{13}C_2]$malate by fumarase, in those cells that had lost plasma membrane integrity.[56]

HP $[1-^{13}C]$fumarate has been obtained from the addition of p-H_2 to $[1-^{13}C]$acetylenedicarboxylic acid (ADC).[10] The attainment of E-alkenes, from catalytic hydrogenation of alkynes, is unusual and their formation derives, mostly, from isomerization of the product of the cis-addition to the triple bond. The complex $[Cp*Ru]^+$ catalyzes the unorthodox formation of the E isomer, thus leading to fumarate, instead of malate, which is the product obtained using conventional hydrogenation complexes. The reaction is quite efficient in aqueous solution, leading to high polarization level ($>24\%$) on the ^{13}C-carboxylate signal and high concentration of the agent. Its metabolic transformation into $[1-^{13}C]$ and $[4-^{13}C]$maleate was observed in cells lysates[57] and in-vivo.[58]

Several other metabolites, or their derivatives, were hyperpolarized by means of PHIP based methods, as reported in different reviews.[59–61] Although the polarization level reported on some of them is good, very few were tested in-vivo. In fact, although the signal enhancement may be sufficient for the in-vitro detection, this is only the first step for identifying a HP molecule as a potential candidate for acting as a diagnostic probe and a sensor for altered metabolic processes.

3.3. Biocompatibility of the solutions of the HP products

The use of a metal complex to exploit the parahydrogen spin order and transforming it into enhanced MR signals is mandatory in both h-PHIP and SABRE. In h-PHIP experiments, rhodium(I) complexes, having the general formula [Rh-(diphos)(diene)]$^+$ (diphos = chelating phosphine) are commonly used, while Crabtree-like Ir(I) complexes are the systems selected for SABRE experiments. A few cases have been reported in which the activation of parahydrogen is obtained by means of organic molecules (i.e. frustrated Lewis pairs),[62] nevertheless their use as hydrogenation catalyst has not been reported yet.

As a prerequisite for clinical trials, the safety profile of any candidate tracer reagent, catalyst and other substances in the product solution has to be carefully assessed. In order to be suitable for in-vivo studies, the osmolarity must be physiological and the concentration of the agent has to be relatively high, in the order of 80–100 mM.

Although it has been shown that the Rh(I) complex used for parahydrogen activation in h-PHIP may be compatible with pre-clinical studies,[63] its removal from the solution of the hyperpolarized product is necessary to obtain solutions suitable for clinical applications. Different methods have been proposed, that can be classifies as filtration, liquid-liquid extraction and precipitation.

When the hydrogenation reaction is carried out in aqueous solution, using a cationic metal complex, filtration of the solution of the hyperpolarized product through a cation-exchange filter[63] appears the most straightforward way to reduce the concentration of the catalyst well below the toxicity level.

Obviously, heterogeneous catalysts are much easier to separate from a reaction mixture than homogeneous ones, therefore routes based on the use of heterogeneous-PHIP (het-PHIP) or het-SABRE has also been considered with the aim of generating catalyst-free hyperpolarized fluids. Metal complexes supported on solids (het-PHIP[64] or het-SABRE[65,66]) and metal particles[67] have been tested. The observed polarization were good in the organic solvents,[68] but significantly lower ($<0.1\%$ on 13 C) when the reactions are carried out in aqueous solution.[50]

Metal scavenging agents have also been proposed to completely eliminate metals from the aqueous solutions of the hyperpolarized products. It was shown that silica particles, functionalized with thiol groups, can precipitate the iridium complexes used in the SABRE experiments, thus allowing to filter off the catalyst.[69]

The liquid-liquid phase extraction is a purification method that has been applied both to h-PHIP[34,9] and SABRE.[70] Hydrogen activation on the metal complex occurs in a lipophilic solvent, such as chloroform, dichloromethane and toluene.[71]

The use of an organic solvent facilitates the hydrogenation reaction thanks to the higher solubility of hydrogen and to the better efficiency of the catalyst. In the h-PHIP experiments, the lipophilic hyperpolarized product, obtained in the organic phase, undergoes a reaction (usually a hydrolysis of an anhydride or an ester) that makes it water-soluble, and the hydrophilic molecule thus obtained is extracted in the aqueous phase. The metal catalyst, being lipophilic, is almost completely retained in the organic phase, while traces of organic solvents may be found in the aqueous phase. Anyhow, these organic solvent residues (toxic) residuals can be removed by means of filtration[46] on a lipophilic resin. It was reported that this latter purification passage causes a decrease of the hyperpolarization which resulted to be about 20% of that observed before filtration.

The liquid-liquid extraction SABRE experiments, named Catalyst Separated Hyperpolarization (CASH) SABRE, rely on the repartition of the substrate between the organic and the aqueous phase.[70] The hyperpolarization substrate is dissolved in the aqueous phase, while the metal complex is in the organic, and the two phases are emulsified, through vigorous shaking, thus allowing an exchange of the substrate between them. Hyperpolarization of the substrate (N-heterocyclic compound) occurs in the organic phase, and hyperpolarization is maintained when it is transferred into the aqueous one. The separation of the two phases takes a few tens of seconds and, being the entire process cyclic, hyperpolarization can be restored, on the product, by successive shakings.

Precipitation of the hyperpolarized molecules from the reaction mixture is another efficient way to remove all the side-compounds (solvents, by-products, catalyst and other reagents) from the hyperpolarized product. This method has been applied for the purification of hyperpolarized $[1-^{13}C]$ fumaric

Analysis & Sensing

Concept
doi.org/10.1002/anse.202200028

Chemistry Europe
European Chemical
Societies Publishing

acid, thanks to its very low solubility in the acidic form, (7 mg/ml, 0.06 M)[72,73] in water. Therefore it was precipitated at acidic pH and then redissolved using an aqueous base. A very important aspect of these experiments was the non-trivial fact that nuclear spin polarization is maintained through phase transitions, provided that the passages from the liquid to the solid state (and vice-versa) takes place in a sufficiently strong magnetic field. In the experiments carried out with HP fumarate, the field provided by a ~100 mT Halbach magnet was sufficient. However it must be noticed that the applicability of this purification strategy is limited by the physicochemical characteristics of the substances.

4. Conclusions and outlook

Hyperpolarization of small molecules in solution provides a powerful tool for in-vivo MRI applications, in particular for the detection of altered metabolic processes in various diseases.

D-DNP is the gold-standard methodology to obtain hyperpolarized molecules in the liquid state, but PHIP can take advantage of the inherent low cost, the higher rate of the polarization cycles and the ease of implementation.

Recently, the advancements in the PHIP-based methods have significantly extended the range of molecules that can be hyperpolarized by means of parahydrogen. Particularly relevant to widen the scope of PHIP appears to be the application of emerging methods such as SABRE-RELAY and PHIP–X.

The routine application of the HP probes obtained by means of PHIP to biological investigations still needs a commercial, dedicated polarizer, although different instrumentations have been developed for PHIP, as reviewed recently.[74]

Limitations to the application of PHIP polarized substrates are still given by the hyperpolarization level and the presence, in some cases, of toxic substances (solvents, catalyst). Therefore further efforts have to be devoted to solve these issues.

Nevertheless, the availability of an affordable HP technique, capable of providing doses of hyperpolarized metabolites suitable for metabolic investigations at a preclinical stage, would represent a new powerful tool for research laboratories in the field of drug developments, in the investigation of cancer and of other diseases.

Acknowledgements

Conflict of Interest

The authors declare no conflict of interest.

[1] C. R. Bowers, *Encycl. Magn. Reson.* **2007**, *vol. 9*; 750–769.

[2] J. H. Ardenkjaer-Larsen, B. Fridlund, A. Gram, G. Hansson, L. Hansson, M. H. Lerche, R. Servin, M. Thaning, K. Golman, *Proc. Natl. Acad. Sci. USA* **2003**, *100*, 10158–63.

[3] M. Goldman, *Appl. Magn. Reson.* **2008**, *34*, 219–226.

[4] K. Golman, O. Axelsson, H. Johannesson, S. Månsson, C. Olofsson, J.-S. Petersson, *Magn. Reson. Med.* **2001**, *46*, 1–5.

[5] L. E. Olsson, C. M. Chai, O. Axelsson, M. Karlsson, K. Golman, J. S. Petersson, *Magn. Reson. Med.* **2006**, *55*, 731–737.

[6] F. Reineri, A. Viale, W. Dastrù, R. Gobetto, S. Aime, *Contrast Media Mol. Imaging* **2011**, *6*, 77–84.

[7] T. C. Eisenschmid, R. U. Kirss, P. P. Deutsch, S. I. Hommeltoft, R. Eisenberg, J. Bargon, R. G. Lawler, A. L. Balch, *J. Am. Chem. Soc.* **1987**, *109*, 8089–8091.

[8] C. R. Bowers, D. P. Weitekamp, *J. Am. Chem. Soc.* **1987**, *109*, 5541–5542.

[9] F. Reineri, T. Boi, S. Aime, *Nat. Commun.* **2015**, *6*, 5858.

[10] B. Ripka, J. Eills, H. Kour, M. Leutzsch, M. H. Levitt, K. Munnemann, *Chem Comm* **2018**, *54*, 12246–12249.

[11] A. Farkas, *Orthohydrogen, Parahydrogen and Heavy Hydrogen*, Cambridge University Press, London, **1935**.

[12] H. S. Taylor, H. Diamond, *J. Am. Chem. Soc.* **1935**, *57*, 1251–1256.

[13] C. Bowers, *Phys. Rev. Lett.* **1986**, *57*, 2645–2648.

[14] R. W. Adams, J. A. Aguilar, K. D. Atkinson, M. J. Cowley, P. I. P. Elliott, S. B. Duckett, G. G. R. Green, I. G. Khazal, J. Lopez-Serrano, D. C. Williamson, *Science* **2009**, *323*, 1708–1711.

[15] D. A. Barskiy, S. Knecht, A. V. Yurkovskaya, K. L. Ivanov, *Prog. Nucl. Magn. Reson. Spectrosc.* **2019**, *114–115*, 33–70.

[16] J.-B. Hövener, N. Schwaderlapp, T. Lickert, S. B. Duckett, R. E. Mewis, L. A. R. Highton, S. M. Kenny, G. G. R. Green, D. Leibfritz, J. G. Korvink, et al., *Nat. Commun.* **2013**, *4*, 2946.

[17] M. J. Cowley, R. W. Adams, K. D. Atkinson, M. C. R. Cockett, S. B. Duckett, G. G. R. Green, J. A. B. Lohman, R. Kerssebaum, D. Kilgour, R. E. Mewis, *J. Am. Chem. Soc.* **2011**, *133*, 6134–6137.

[18] D. Canet, C. Aroulanda, P. Mutzenhardt, S. Aime, R. Gobetto, F. Reineri, *Concepts Magn. Reson. Part A* **2006**, *28*, DOI 10.1002/cmr.a.20065.

[19] M. G. Pravica, D. P. Weitekamp, *Chem. Phys. Lett.* **1988**, *145*, 255–258.

[20] G. Pileio, *Prog. Nucl. Magn. Reson. Spectrosc.* **2017**, *98–99*, 1–19.

[21] J. Barkemeyer, M. Haake, J. Bargon, *J. Am. Chem. Soc.* **1995**, *117*, 2927–2928.

[22] G. Stevanato, J. Eills, C. Bengs, G. Pileio, *J. Magn. Reson.* **2017**, *277*, 169–178.

[23] H. Jóhannesson, O. Axelsson, M. Karlsson, *Comptes Rendus Phys.* **2004**, *5*, 315–324.

[24] M. Goldman, H. Jóhannesson, *Comptes Rendus Phys.* **2005**, *6*, 575–581.

[25] S. Kadlecek, K. Emami, M. Ishii, R. Rizi, *J. Magn. Reson.* **2010**, *205*, 9–13.

[26] J. Eills, G. Stevanato, C. Bengs, S. Glöggler, S. J. Elliott, J. Alonso-valdesueiro, G. Pileio, M. H. Levitt, *J. Magn. Reson.* **2017**, *274*, 163–172.

[27] S. Bär, T. Lange, D. Leibfritz, J. Hennig, D. Von Elverfeldt, J. B. Hövener, *J. Magn. Reson.* **2012**, *225*, 25–35.

[28] S. Kinner, S. Maderwald, N. Parohl, J. Albert, C. Corot, P. Robert, B. Jorg, F. M. Vogt, *Invest. Radiol.* **2011**, *46*, 254–259.

[29] https://www.federalregister.gov/documents/2017/01/11/2016-31262/national-primary-drinking-water-regulations-announcement-of-the-results-of-epas-review-of-existing, **2016**.

[30] M. Goldman, H. Jóhannesson, O. Axelsson, M. Karlsson, in *Magn. Reson. Imaging*, **2005**, pp. 153–157.

[31] P. Bhattacharya, E. Y. Chekmenev, W. H. Perman, K. C. Harris, A. P. Lin, V. A. Norton, C. T. Tan, B. D. Ross, D. P. Weitekamp, *J. Magn. Reson.* **2007**, *186*, 150–155.

[32] E. Y. Chekmenev, J. Hövener, V. A. Norton, K. Harris, L. S. Batchelder, P. Bhattacharya, B. D. Ross, D. P. Weitekamp, *J. Am. Chem. Soc.* **2008**, *130*, 4212–4213.

[33] J. B. Hövener, E. Y. Chekmenev, K. C. Harris, W. H. Perman, L. W. Robertson, B. D. Ross, P. Bhattacharya, *Magn. Reson. Mater. Phys.* **2009**, *22*, 111–121.

[34] F. Reineri, A. Viale, S. Ellena, T. Boi, V. Daniele, R. Gobetto, S. Aime, *Angew. Chem. Int. Ed.* **2011**, *50*, 7350–7353; *Angew. Chem.* **2011**, *123*, 7488–7491.

[35] C. Von Morze, P. E. Z. Larson, S. Hu, K. Keshari, D. M. Wilson, J. H. Ardenkjaer-Larsen, A. Goga, R. Bok, J. Kurhanewicz, D. B. Vigneron, *J. Magn. Reson. Imaging* **2011**, *33*, 692–697.

[36] W. Iali, P. J. Rayner, S. B. Duckett, *Sci. Adv.* **2018**, *4*, 1–7.

[37] K. R. Keshari, D. M. Wilson, Chemistry and Biochemistry of 13 C Hyper-polarized Magnetic Resonance Using Dynamic Nuclear Polarization., **2014**.

[38] S. J. Nelson, J. Kurhanewicz, D. B. Vigneron, P. E. Z. Larson, A. L. Harzstark, M. Ferrone, M. Van Criekinge, J. W. Chang, R. Bok, I. Park, et al., *Sci. Transl. Med.* **2013**, *5*, 198ra108.

[39] J. H. Ardenkjaer-Larsen, *J. Magn. Reson.* **2019**, *306*, 124–127.

[40] L. S. Lloyd, A. Asghar, M. J. Burns, A. Charlton, S. Coombes, M. J. Cowley, G. J. Dear, S. B. Duckett, G. R. Genov, G. G. R. Green, et al., *Catal. Sci. Technol.* **2014**, *4*, 3544–3554.

[41] A. J. Holmes, P. J. Rayner, M. J. Cowley, G. G. R. Green, A. C. Whitwood, S. B. Duckett, *Dalton Trans.* **2014**, *44*, 1077–1083.

[42] W. Iali, S. S. Roy, B. J. Tickner, F. Ahwal, A. J. Kennerley, S. B. Duckett, *Angew. Chem. Int. Ed.* **2019**, *58*, 10271–10275; *Angew. Chem.* **2019**, *131*, 10377–10381.

[43] B. J. Tickner, O. Semenova, W. Iali, P. J. Rayner, A. C. Whitwood, S. B. Duckett, *Catal. Sci. Technol.* **2020**, *10*, 1343–1355.

[44] I. Adelabu, P. Tomhon, M. S. H. Kabir, S. Nantogma, M. Abdulmojeed, I. Mandzhieva, J. Ettedgui, R. E. Swenson, M. C. Krishna, T. Theis, et al., *Chem Phys Chem* **2022**, *23*, 131–136.

[45] B. J. Tickner, P. J. Rayner, S. B. Duckett, *Anal. Chem.* **2020**, *92*, 9095–9103.

[46] O. Bondar, E. Cavallari, C. Carrera, S. Aime, F. Reineri, *Catal. Today* **2021**, *397–399*, 94–102, DOI 10.1016/j.cattod.2021.11.030.

[47] E. Cavallari, C. Carrera, M. Sorge, G. Bonne, A. Muchir, S. Aime, F. Reineri, *Sci. Rep.* **2018**, *8*, 8366.

[48] E. Cavallari, C. Carrera, S. Aime, F. Reineri, *ChemPhysChem* **2019**, *20*, 318–325.

[49] E. Cavallari, C. Carrera, G. Di Matteo, O. Bondar, S. Aime, F. Reineri, *Front. Oncol.* **2020**, *10*, 497.

[50] K. V. Kovtunov, D. A. Barskiy, R. V. Shchepin, O. G. Salnikov, I. P. Prosvirin, A. V. Bukhtiyarov, L. M. Kovtunova, V. I. Bukhtiyarov, I. V. Koptyug, E. Y. Chekmenev, *Chem. A Eur. J.* **2016**, *22*, 16446–16449.

[51] E. Cavallari, C. Carrera, S. Aime, F. Reineri, *Chem. A Eur. J.* **2017**, *23*, 1200–1204.

[52] L. Kaltschnee, A. P. Jagtap, J. McCormick, S. Wagner, L. S. Bouchard, M. Utz, C. Griesinger, S. Glöggler, *Chem. A Eur. J.* **2019**, *25*, 11031–11035.

[53] A. N. Pravdivtsev, G. Buntkowsky, S. B. Duckett, I. V. Koptyug, J. B. Hövener, *Angew. Chem. Int. Ed.* **2021**, *60*, 23496–23507.

[54] T. Trantzschel, M. Plaumann, J. Bernarding, D. Lego, T. Ratajczyk, S. Dillenberger, G. Buntkowsky, J. Bargon, U. Bommerich, *Appl. Magn. Reson.* **2013**, *44*, 267–278.

[55] S. Glöggler, R. Müller, J. Colell, M. Emondts, M. Dabrowski, B. Blümich, S. Appelt, *Phys. Chem. Chem. Phys.* **2011**, *13*, 13759.

[56] F. A. Gallagher, M. I. Kettunen, D.-E. Hu, P. R. Jensen, R. In't Zandt, M. Karlsson, A. Gisselsson, S. K. Nelson, T. H. Witney, S. E. Bohndiek, et al., *PNAS* **2009**, *106*, 19801–19806.

[57] J. Eills, E. Cavallari, C. Carrera, D. Budker, S. Aime, F. Reineri, *J. Am. Chem. Soc.* **2019**, *141*, 20209–20214.

[58] N. J. Stewart, H. Nakano, S. Sugai, M. Tomohiro, Y. Kase, Y. Uchio, T. Yamaguchi, T. Matsuo, N. Naganuma, N. Takeda, et al., *ChemPhysChem* **2021**, *22*, 915–923.

[59] F. Reineri, E. Cavallari, C. Carrera, S. Aime, *Magn. Reson. Mater. Phys. Biol. Med.* **2021**, *34*, 25–47.

[60] A. J. Hovener, A. N. Pravdivtsev, B. Kidd, R. Bowers, S. Glöggler, K. V. Kovtunov, R. Katz-Brull, K. Buckenmaier, F. Reineri, T. Theis, et al., *Angew. Chem. Int. Ed.* **2018**, *57*, 11140–11162; *Angew. Chem.* **2018**, *130*, 11310–11333.

[61] G. Buntkowsky, F. Theiss, J. Lins, Y. A. Miloslavina, L. Wienands, A. Kiryutin, A. Yurkovskaya, *RCS Adv.* **2022**, *12*, 12477–12506.

[62] K. Sorochkina, V. V. Zhivonitko, K. Chernichenko, V. V. Telkki, T. Repo, I. V. Koptyug, *J. Phys. Chem. Lett.* **2018**, *9*, 903–907.

[63] H. Chan, P. Bhattacharya, A. Imam, A. Freundlich, T. Tran, W. Perman, A. Lin, K. Harris, E. Chekmenev, M. Ingram, et al., *Proc. 17th Sci. Meet. Int. Soc. Magn. Reson. Med.* **2009**, *Honolulu*, 2448.

[64] L. S. Bouchard, S. R. Burt, M. S. Anwar, K. V. Kovtunov, I. V. Koptyug, A. Pines, *Science* **2008**, *319*, 442–445.

[65] F. Shi, A. M. Coffey, K. W. Waddell, E. Y. Chekmenev, B. M. Goodson, *Angew. Chem. Int. Ed.* **2014**, *53*, 7495–7498; *Angew. Chem.* **2014**, *126*, 7625–7628.

[66] K. V. Kovtunov, L. M. Kovtunova, M. E. Gemeinhardt, A. V. Bukhtiyarov, J. Gesiorski, V. I. Bukhtiyarov, E. Y. Chekmenev, I. V. Koptyug, B. M. Goodson, *Angew. Chem. Int. Ed.* **2017**, *56*, 10433–10437; *Angew. Chem.* **2017**, *129*, 10569–10573.

[67] K. V. Kovtunov, I.E. Beck, V. I. Bukhtiyarov, I. V. Koptyug, *Angew. Chem. Int. Ed.* **2008**, *47*, 1492–1495; *Angew. Chem.* **2008**, *120*, 1514–1517.

[68] S. Korchak, S. Mamone, S. Glçggler, *Chem. Open* **2018**, *7*, 672–676.

[69] D. A. Barskiy, L. A. Ke, X. Li, V. Stevenson, N. Widarman, H. Zhang, A. Truxal, A. Pines, *J. Phys. Chem. Lett.* **2018**, *9*, 2721–2724.

[70] W. Iali, A. M. Olaru, G. G. R. Green, S. B. Duckett, *Chem. A Eur. J.* **2017**, *23*, 10491–10495.

[71] O. Bondar, E. Cavallari, C. Carrera, S. Aime, F. Reineri, *Catal. Today* **2022**, *397–399*, 94–102.

[72] J. Eills, J. Alonso-valdesueiro, E. S. Marcano, J. Ferreira, S. Alom, G. J. Rees, J. V. Hanna, M. Carravetta, M. H. Levitt, *ChemPhysChem* **2018**, *19*, 40–44.

[73] S. Knecht, J. W. Blanchard, D. Barskiy, E. Cavallari, L. Dagys, E. van Dyke, M. Tsukanov, B. Bliemel, K. Münnemann, S. Aime, et al., *Proc. Natl. Acad. Sci. USA* **2021**, *118*, 1–6.

[74] A. B. Schmidt, C. R. Bowers, K. Buckenmaier, E. Y. Chekmenev, H. de Maissin, J. Eills, F. Ellermann, S. Glöggler, J. W. Gordon, S. Knecht, et al., *Anal. Chem.* **2022**, *94*, 479-501DOI 10.1021/acs.analchem.1c04863.